Scientific Utility of the Signal-to-Noise Ratio (SNR) Reported by Geodetic GPS Receivers

Andria Bilich*, Penina Axelrad and Kristine M. Larson
University of Colorado, Dept. of Aerospace Engineering Sciences
* now at the National Geodetic Survey

BIOGRAPHY

Andria Bilich is a geodesist with the National Geodetic Survey's Geosciences Research Division. Her research interests include GPS multipath characterization and precision improvements to high-rate (1-Hz) positioning for geoscience applications. She received her B.S. in geophysics (1999) from the University of Texas and Ph.D. in aerospace engineering (2006) from the University of Colorado.

Penina Axelrad is Professor of Aerospace Engineering Sciences with the Colorado Center for Astrodynamics Research at the University of Colorado, Boulder. Her research interests are in GPS technology and applications to aerospace systems. She has been involved in GPS work since 1985 and is a past president of the ION.

Kristine M. Larson received a B.A. in Engineering Sciences from Harvard and a Ph.D. in Geophysics from the University of California, San Diego. Her research focuses on high-precision applications of GPS, including plate tectonics, volcano monitoring, seismology, and time transfer. She is currently Professor of Aerospace Engineering Sciences at the University of Colorado.

ABSTRACT

Although GPS signal-to-noise ratio (SNR) measurements have conventionally been used only as a measure of receiver tracking or signal strength comparison between channels, new scientific applications of SNR are evolving. These scientific applications exploit the link between oscillations in SNR and carrier phase multipath under the simplified model of the receiver response to tracking a composite signal of direct plus reflected signals. This paper establishes several principles linking dual-frequency SNR data, pseudorange multipath, and phase multipath, and uses these principles to test the dependency of SNR data on the simplified multipath model for several common models of geodetic-quality receivers. SNR data from AOA ACT receivers pass these tests and demonstrate a strong link to the model, and we provide several examples of SNR-multipath science applications that can be done when SNR data are deemed to be reliable and accurate. Examples are drawn from permanent stations operating ACT receivers and include multipath map formation, construction of carrier phase multipath corrections, and soil moisture monitoring examples. However, perhaps because of the lack of requirements established for SNR measurements, we find considerable inconsistency among manufacturers and models and show that most geodetic receivers report SNR data in a way that obscures or misrepresents the multipath signature. Problematic characteristics observed in some receivers' SNR data include strong coupling of L1 and L2 tracking errors, apparent oscillations unrelated to the multipath environment, coarse values, or data correlations inconsistent with the multipath model. Our findings suggest that changes to SNR reporting to establish a consistent and reliable measurement could greatly enhance the scientific utility of existing GPS networks.

INTRODUCTION

In addition to carrier phase and code observables, GPS receivers routinely record signal-to-noise ratios or SNR. As the term indicates, SNR is a ratio of signal power to the noise floor of the GPS observation, and has conventionally been used only as a measure of receiver tracking efficacy or for comparison of signal strengths between channels and satellites. When SNR are calculated from the prompt accumulations of the code tracking loop [*Ward*, 1996], the measured SNR are directly related to carrier phase errors due to multipath [*Braasch*, 1996; *Comp and Axelrad*, 1997; *Axelrad et al*., 2005]. Multipath error on code and carrier measurements is of concern as specular multipath remains a major uncorrected error source in GPS measurements, and is consequently a source of active research. New scientific applications of SNR data are evolving out of this multipath research that exploit the link between oscillations in SNR and carrier phase multipath. Thus, with reliable and consistent SNR data, current networks

now used only for positioning purposes may become useful for other scientific applications.

Our study analyzes the SNR data quality and utility for scientific applications for some models of Allen-Osborne, Ashtech, Javad, Leica, and Trimble dual-frequency receivers. We concentrate on select receiver models that are common in CGPS geodetic networks; as these data are publicly available and often archived for years for globally distributed stations, CGPS geodetic networks provide a spatially and temporally rich data set for research purposes.

SNR data are routinely recorded by GPS receivers but are less frequently reported in RINEX data files [*Gurtner and Mader*, 1990]. When available in RINEX, these data are reported as observable types S1 and S2, and record "raw signal strengths or SNR values as given by the receiver for L1, L2 phase observations." The RINEX translation software TEQC [*Estey and Meertens*, 1999] now reports SNR in dB (power or amplitude) for the majority of common GPS geodetic receivers. However, how these quantities are actually computed and the native units of these measurements vary depending on the receiver manufacturer and receiver model, and are often proprietary. Thus it is difficult to confirm which GPS receiver models compute and report SNR in a way that is consistent with established multipath relationships and therefore useful for scientific study.

The following section outlines the well-known simplified model of the receiver response to tracking a composite signal of direct plus reflected signals. We motivate our study of SNR quality by providing examples of SNR-multipath science applications that can be done when SNR data are deemed to be reliable and accurate. We then identify which receiver models produce SNR observations most consistent with the simplified multipath model as a test of SNR applicability to multipath research, and identify problems that make some receivers' SNR data of doubtful utility.

SNR THEORY

SNR is an observable commonly recorded by GPS receivers that is sensitive to carrier phase multipath. In this section we summarize some key SNR, carrier, and code multipath relationships which are used to assess SNR data quality for scientific purposes; the reader is directed to the extensive derivations in [*Georgiadou and Kleusberg*, 1988; *Axelrad et al*., 2005; *Bilich and Larson*, 2007] for additional background.

In many GPS receivers, SNR is derived from the carrier tracking loop outputs and is recorded for each GPS frequency. The below relationships assume that SNR is a direct measure of the prompt accumulation of the carrier tracking loop normalized by some noise factor. We describe carrier loop operation and the magnitude of the prompt correlation through a phasor representation of signal tracking with in-phase and quadrature channels (Figure 1). This discussion assumes specular reflections from surfaces that are large compared to the signal wavelength (~19 cm for L1 and 24 cm for L2 GPS signals). This model only applies in the far field where the distance between antenna and reflector is more than a few wavelengths; the applicability of the results to close-in reflectors is not guaranteed.

Under proper carrier loop operation and a multipath-free environment, SNR is equivalent to the magnitude of the direct signal A_d. When one or more multipath signals are introduced, the carrier tracking loop attempts to track a composite signal; the SNR then becomes a measurement of composite signal amplitude. The SNR that includes a single reflected (multipath) signal of amplitude A_m can be expressed as

$$SNR^2 = A_d^2 + A_m^2 + 2A_d A_m \cos\psi \qquad (1)$$

where ψ is the multipath relative phase, an arbitrary phase offset of the reflected signal from the direct which incorporates both the physical path delay of the signal as well as a phase shift that occurs with reflection. Also when tracking a composite signal, the true carrier phase is biased by the phase error due to multipath ϕ_{MP}:

$$\tan\phi_{MP} = \frac{A_m \sin\psi}{A_d + A_m \cos\psi} \qquad (2)$$

Both of these equations are easily derived from the phasor diagram (Figure 1), and can be extended to include summation terms for multiple reflections. Through these equations SNR, an observable and measurable quantity, is directly related to the carrier phase error due to multipath, a quantity that cannot be directly measured from the carrier observable.

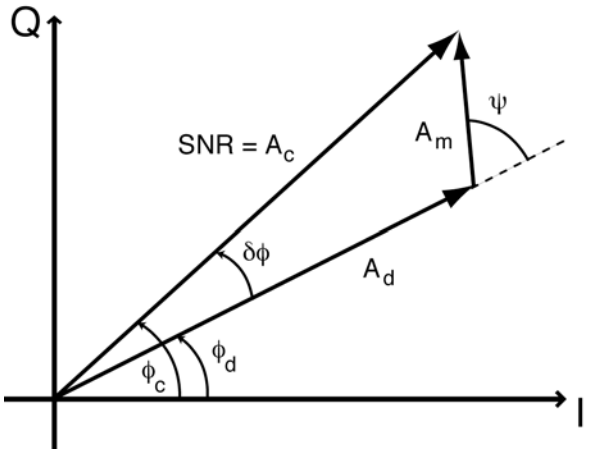

Figure 1: Phasor diagram for in-phase (I) and quadrature (Q) channels, describing the relationship between the amplitudes of the direct (A_d), multipath (A_m), and composite (A_c) signals and their phases – multipath relative phase ψ and carrier phase error $\delta\phi$ (denoted ϕ_{MP} in Equation 2).

Similar relationships exist to link multipath pseudorange error to multipath parameters and measurable quantities. From the ideal code tracking loop discriminator equation and the assumption of short delay multipath [*Axelrad et al.*, 2005; *Braasch*, 1996], the pseudorange multipath error ρ_{MP} is written as:

$$\rho_{MP} = \frac{\alpha\delta\cos\psi}{1+\alpha\cos\psi} \quad (3)$$

where α is the ratio of multipath and direct amplitudes (A_m/A_d) and δ is the path delay, i.e. the additional path length traveled by a reflected signal relative to the direct. We relate ρ_{MP} to an observable quantity, the pseudorange (code) multipath observable, which is a function of the measured pseudorange ρ and the measured carrier phases on L1 and L2 (ϕ_1 and ϕ_2). Forming this combination for L1 code multipath (*MP1*), we see that this observable is a function of the code error, a constant C due to the phase ambiguities, and the code tracking noise ε_ρ, i.e.:

$$MP1 = \rho_{MP} + C + \varepsilon_\rho \quad (4)$$

This observable combination can be written for each GPS frequency, thereby linking the code multipath observable to the code error due to multipath. In these equations, all terms vary with time but the time-dependence is omitted for clarity. Note that the amplitude terms include receiving antenna gain pattern effects and indirect signal attenuation upon reflection; thus, for the majority of geodetic GPS antennas and multipath-generating geometries, $A_m(t) << A_d(t)$.

In Equations 1-4, multipath relative phase serves as the common and dominant time-varying term. Assuming a static environment with antenna and reflecting objects that do not move, the multipath relative phase will change with motion of the broadcasting GPS satellite. This motion leads to oscillations in SNR, multipath phase error, and multipath pseudorange error, all of which are dominated by the sine or cosine of ψ [*Axelrad et al.*, 2005]. If we consider the time-varying nature of ψ with respect to satellite elevation angle θ for a reflecting object at distance h, the corresponding multipath frequency ω is given by:

$$\omega \equiv \frac{d\psi}{dt} = \frac{2\pi}{\lambda} 2h\cos\theta\frac{d\theta}{dt} \quad (5)$$

It is the time-varying nature of these quantities which allows us to understand the links between observables and errors, and how this time-varying signature is a function of the GPS carrier frequency. First, we note common $\cos\psi$ terms in *SNR* and ρ_{MP} (Equations 1 and 3), and surmise that oscillations in the SNR and the code multipath combination on the same GPS frequency should be in-phase. Second, multipath frequency (Equation 5) is a function of the GPS carrier wavelength; assuming that the same multipath geometry (θ and h) affects L1 and L2 signals simultaneously, the subsequent time-varying signatures of S1 and S2 will be different. In this case the frequency of S1 and S2 oscillations will differ by the inverse ratio of their respective carrier wavelengths, i.e. $\omega_1/\omega_2 \approx \lambda_{L2}/\lambda_{L1}$ = 1.283, leading to SNR time series which are largely out-of-phase with each other and have localized frequency content of a defined ratio.

To test the dependency of SNR data on the simplified multipath model, we examine the time-varying signatures of *SNR* and *MP*. First, we visually inspect SNR data from each receiver for anomalies, and assess any limitations imposed by precision of reported data. Second, we establish the phase relationship between data types through cross-correlation and use the shorthand $C_{A/B}(t) = corr\big(A(t),B(t)\big)$ to denote the cross-correlation of two data types A and B. Before computing the correlation, we normalize each series so the auto-correlations at zero lag are identically 1.0, facilitating correlation comparisons for different data types and receivers with different SNR units. Finally, we compute localized estimates of frequency content for each time series to establish frequency relationships between S1 and S2 data types. Using these criteria (summarized in Table 1), we identify which receiver models produce SNR observations most consistent with the simplified multipath model, and provide examples of scientific applications of these data. If some of these relationships fail, then the link between SNR and multipath is poorly defined and consequently limits the utility of these SNR data for scientific applications.

HIGH UTILITY SNR

We begin by exploring the scientific utility of SNR from Allen-Osborne Benchmark ACT receivers. These models calculate and report a receiver voltage SNR, which is the peak signal voltage divided by the root-mean-square (RMS) of the noise voltage [Larry Young, personal communication]. The signal voltage is the accumulation (or integration) of the prompt correlator output; the noise voltage is the square root of the number of samples correlated scaled to one second. Viewed in phasor space (Figure 1), SNR for this receiver is equivalent to the amplitude of the direct phasor (A_d) in the multipath-free case or the composite phasor in the multipath-corrupted case (A_c), and should obey the assumptions of the simplified multipath model.

To demonstrate how SNR from AOA Benchmark ACT receivers obey the above multipath assumptions, we present data from two different stations operating Benchmark ACT receivers: CHUR in Churchill, Canada and TASH in Tashkent, Uzbekistan. Both sites have 1-Hz data available through the International GNSS Service archives (ftp://cddis.gsfc.nasa.gov/gps/data/highrate/) and use AOA D/M_T chokering antennas, but are situated in

very different multipath environments: TASH is atop a ~5.0m concrete pillar in a flat field (Figure 2), while CHUR is on a ~1.5m pillar above undulating ground with rocky outcrops (Figure 3).

The different antenna-ground distances result in very different dominant frequencies of oscillation in the SNR data (Figures 4a-b, 5a-b). Despite the disparate multipath environments and constituent frequencies, both stations' data satisfy all the conditions set forward in Table 1. First, visual inspection of the SNR data shows that they are sufficiently precise so that oscillations vary smoothly. Second, at each station the SNR and MP observables on the same GPS frequency are in-phase and have the same frequency content, as shown by data cross-correlations (Figures 4c, 5c) and power spectra (Figures 4d, 5d), respectively. The cross-correlations have peak values at zero lag with relatively narrow correlation peak width. Finally, SNR on the different GPS frequencies (S1 and S2) are uncorrelated and, during the high amplitude time periods examined, have dominant frequencies of the appropriate ratio expected for the GPS wavelengths, i.e. $\omega_{S1}/\omega_{S2} \approx 1.28$ (Figures 4d, 5d).

Table 1: Expected relationships between recorded SNR data (*SNR*) and the pseudorange (code) multipath combination (*MP*) for data obeying the simplified multipath model of receiver response to tracking a composite signal of direct plus reflected signals.

Expected relationship	Explanation
Smoothly-varying *S1(t)*, *S2(t)*	*S1*, *S2* data of sufficient precision and lacking anomalous values which could be misconstrued as multipath
$\max\left(C_{S1/MP1}(t)\right) = C_{S1/MP1}(0)$	*S1(t)* and *MP1(t)* have maximum correlation at zero lag
$\max\left(C_{S2/MP2}(t)\right) = C_{S2/MP2}(0)$	*S2(t)* and *MP2(t)* have maximum correlation at zero lag
$C_{S1/S2}(t) << C_{S1/MP1}(0), C_{S2/MP2}(0)$	*S1(t)* and *S2(t)* are uncorrelated, i.e. do not have a sharp correlation peak at zero lag
$f_{S1}/f_{S2} = \lambda_{L2}/\lambda_{L1} \approx 1.28$	Dominant frequencies present in *S1(t)* and *S2(t)* obey the ratio of their carrier wavelengths

Figure 2: Site photographs of TASH, Tashkent, Uzbekistan, with the GPS antenna located on the ~ 5.0m pillar in the center of each photograph. Photos from GFZ, http://www.gfz-potsdam.de/pb1/igs/igs_stat/tash_photo.htm

Figure 3: Site photographs of CHUR, Churchill, Manitoba, with the GPS antenna located on the ~1.5m tall pillar in both photos. Left: view to the north and Hudson Bay. Right: view to the south with metal building.

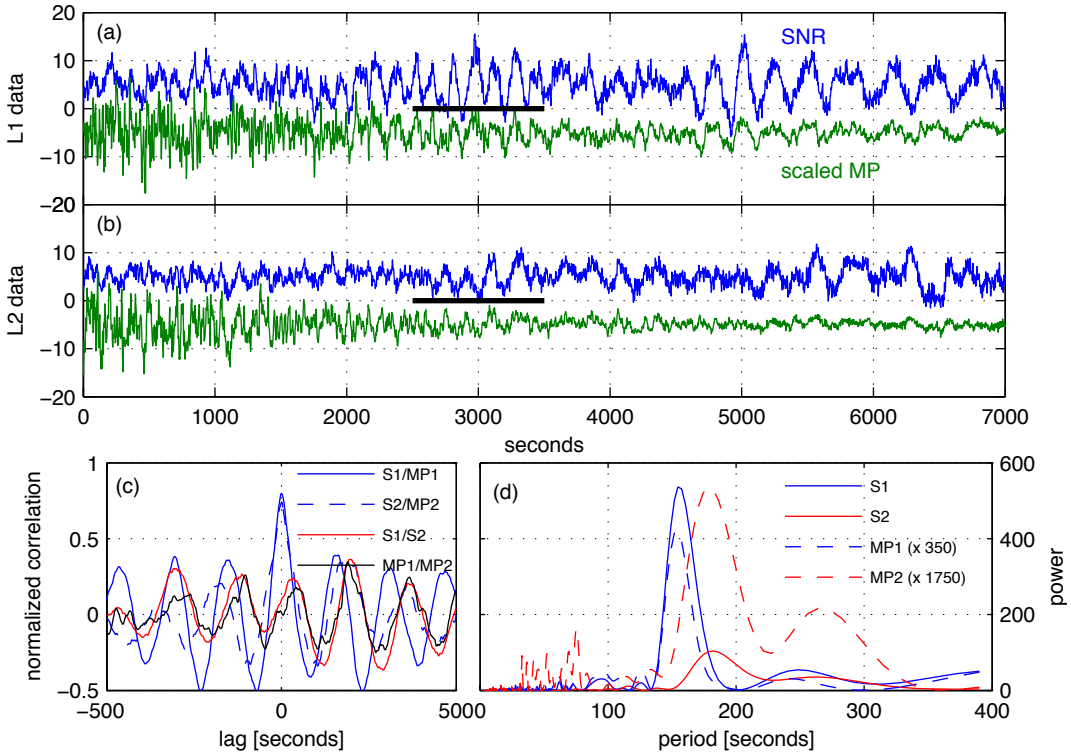

Figure 4: SNR and code multipath combination data from the ascending arc of PRN14 as observed from TASH on 2007 January 1. SNR data (V) and code multipath combination (meters x10) as a function of time for L1 (a) and L2 (b) frequencies. Both data types have been lowpass filtered for >6s periods to minimize noise, and the direct signal amplitude has been removed from the SNR time series. (c) Cross-correlation of a subset of data (2500-3500s, covering 39-47° elevation) indicated by the heavy line in (a-b), where data were normalized to yield unity autocorrelation at zero lag; (d) spectral power of the same 1000s examined in (b), with units m^2/Hz (multipath combination) and V^2/Hz (SNR).

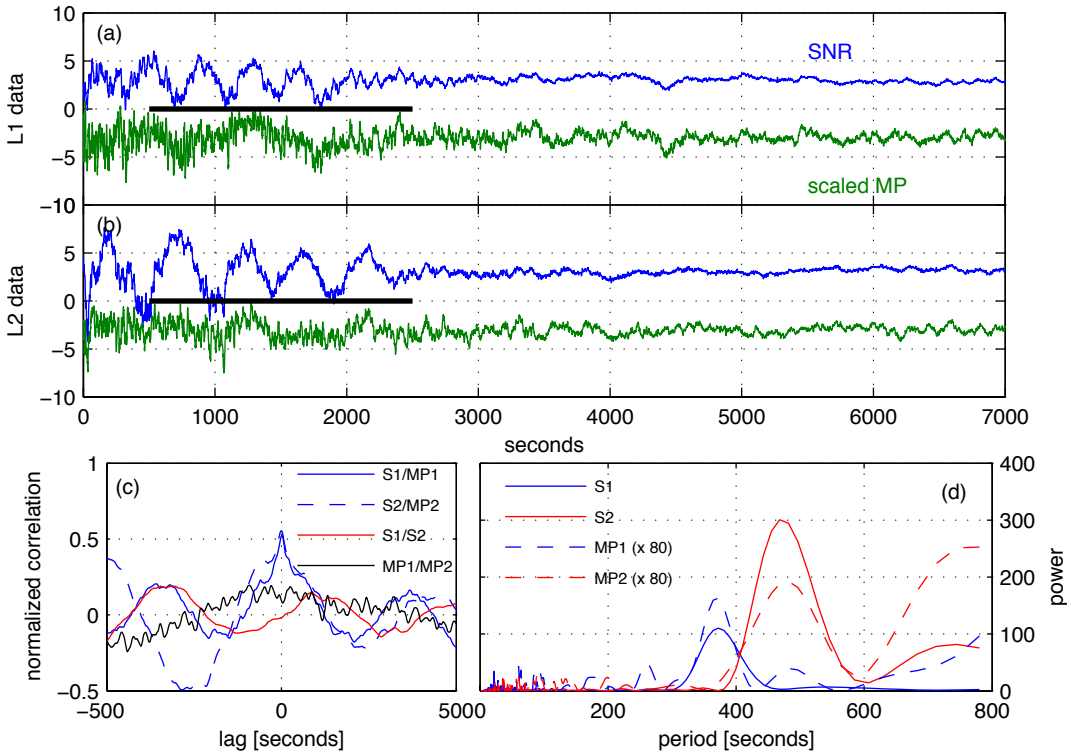

Figure 5: SNR and code multipath combination data from the ascending arc of PRN7 as observed from CHUR on 2006 August 1; data were lowpass filtered for >5s periods and MP have units of meters (scaled x3); see Figure 4 for subplot explanations. Plots (c) and (d) use the 500-2500s of data marked by the heavy line in (a-b), which cover 17-29° elevation.

Because these receivers have SNR with exemplary qualities – good resolution of multipath amplitude and phase with good correspondence to the simplified multipath model – these data can be used in scientific study to great advantage. We present examples of power spectral mapping [*Bilich and Larson*, 2007] and phase error modeling [e.g. *Bilich et al.*, 2007; *Comp and Axelrad*, 1998] using SNR data from CHUR on 2006 August 1, and an example of soil moisture monitoring from TASH [*Larson et. al*, 2007]. Data from non-winter months are used to avoid snow effects (both snow on the ground and on top of the antenna) and concentrate on multipath from local topography and adjacent structures.

With quality SNR data, one can use localized estimates of SNR frequency and amplitude to understand the multipath environment by forming power spectral maps [*Bilich and Larson*, 2007]. In this technique, the wavelet transform [*Torrence and Compo*, 1998] is used to extract time-varying estimates of multipath frequency and amplitude for each satellite in view; these data are examined in a spectral band of interest and projected onto a sky plot depicting the multipath characteristics of a GPS site. Examining SNR data in frequency bands allows the analyst to determine the approximate distance to reflecting objects (Equation 5), then use satellite elevation and azimuth information to pinpoint the object's likely direction. As an example, power spectral maps for CHUR on 2006 August 1 (Figure 6) demonstrate interesting spatial patterns of high-amplitude multipath. For both GPS frequencies, strong returns are observed for satellites at 30-60° elevation to the S and SSE. The relatively short periods (100-300s) are consistent with a reflecting object ~6m away, the approximate location of a building with a sloped roof and a tall rock outcropping (Figure 3). Although the exact orientation and slope of these objects has not been measured, it is plausible that these objects are the source of observed multipath reflections. Additionally, strong returns are observed at slightly longer periods (300-500s) primarily at shallow satellite elevation angles, consistent with the ~2m distance between the ground and the antenna phase center. The discrete nature of the strong returns and range of possible periods indicates that the different sloped rock outcroppings serve has multipath reflectors of differing effective height h. It is interesting to note that similar but not identical patterns of strong returns are observed in both S1 and S2 power spectral maps, potentially due to the lower hemisphere antenna pattern differences for L1 and L2 signals.

With a related technique, it is possible to extract carrier phase multipath corrections from SNR frequency and amplitude. As demonstrated for multi-antenna arrays [*Comp and Axelrad*, 1998; *Ray*, 2000] and single stations [*Bilich*, 2006; *Bilich et al*., 2007], multipath spectral parameters (frequency, amplitude, and phase offset) as captured by the SNR can be used to construct a profile of multipath error in the carrier phase. When applied to the original carrier phase data, the profile removes systematic errors due to multipath from phase measurements and results in more accurate position estimates. This technique relies upon a direct relationship between carrier phase multipath and SNR oscillations (Equations 1 and 2), and therefore requires SNR data which obey the simplified multipath model in order to correctly extract multipath parameters and remove multipath errors. In Figure 7, SNR data recorded for PRN16 at CHUR show distinct oscillations on both L1 and L2 data streams. Using the technique of *Bilich et al*. [2007], the SNR due to multipath δSNR is modeled to determine direct and multipath amplitudes and the multipath relative phase. These parameters are combined (Equation 2) to yield a carrier phase multipath correction for each GPS frequency. The ionosphere-free combination of the single-frequency corrections is in-phase and possesses similar amplitudes to point positioning postfit residuals (Figure 7, bottom). An exact correspondence is not expected due to the likely least-squares distribution of errors amongst satellites in the solution. As shown in *Bilich et al*. [2007], phase corrections derived from reliable SNR data are capable of removing phase multipath error and would yield whitened ppp residuals in the example shown here.

Finally, it is possible to use changes in multipath signal amplitude over time as a proxy for soil moisture content. In the technique described by *Larson et al.* [2007], incoming signals are reflected from and attenuated by the ground before reception by the GPS antenna. The amplitude of SNR oscillations largely depends on surface reflectivity because the surface dielectric constant is strongly coupled to soil moisture content in the upper few centimeters of the ground. Thus, if a fixed area (i.e. fixed satellite-receiver geometry) is sensed by the reflected signal, changes in that signal's amplitude will mirror changes in near-surface soil moisture. Consider an example from *Larson et al.* [2007] for observations at TASH over 35 days in 2005 (Figure 8). With each significant rain event, the multipath amplitude suddenly increases then gradually decreases over subsequent days as the soil dries out. In this study, multipath amplitudes for two satellites sensing the same section of ground demonstrate comparable trends to modeled volumetric water content in the top 5cm of the water column.

These examples show that SNR data, when consistent with the simplified multipath model and reported with sufficient precision, contain information about the multipath environment and how reflected signals contribute to errors in GPS positioning. However, as the following section shows, SNR data reported by various geodetic GPS receivers have characteristics which detract from their potential for scientific study.

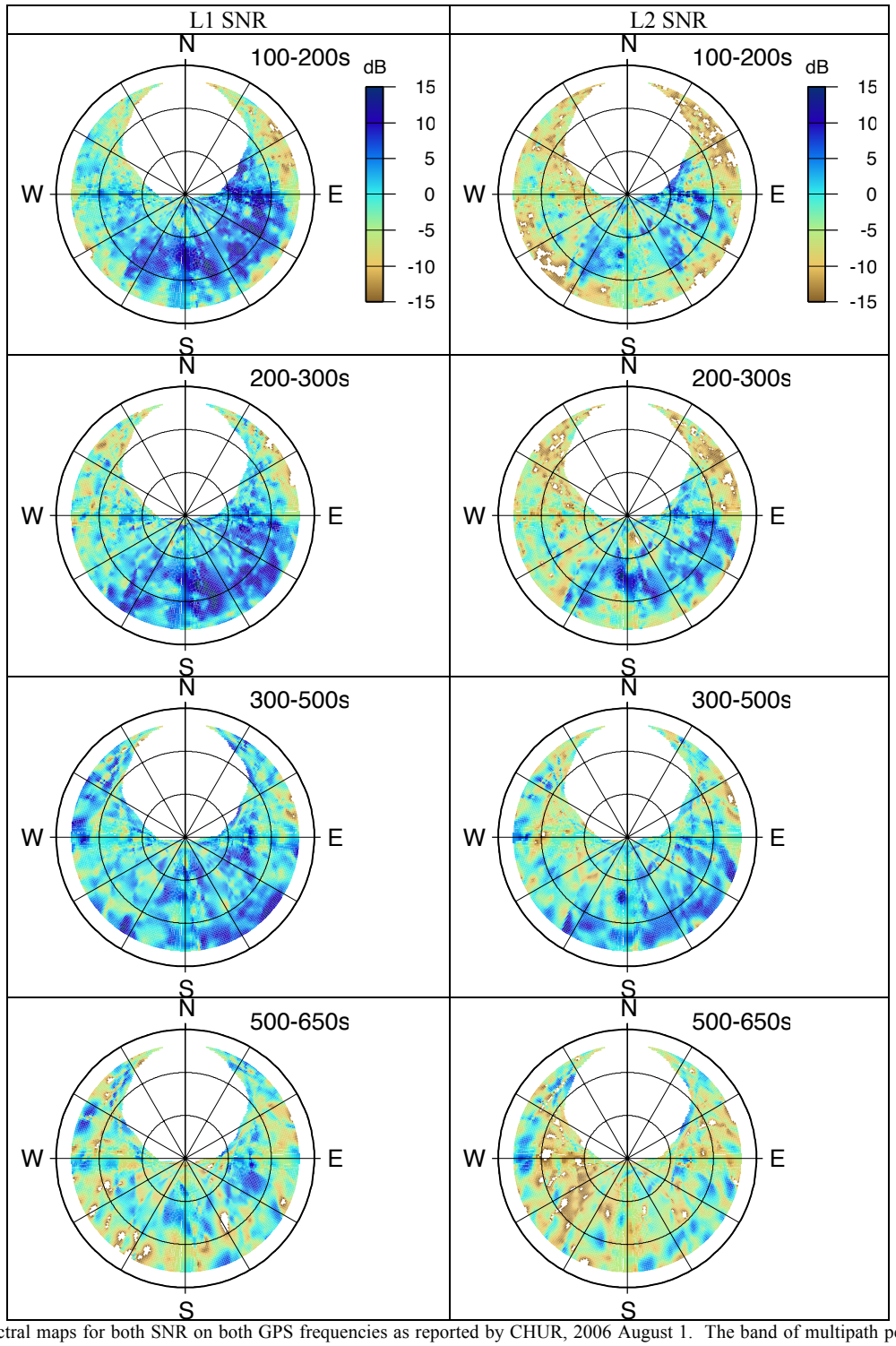

Figure 6: Power spectral maps for both SNR on both GPS frequencies as reported by CHUR, 2006 August 1. The band of multipath periods examined is given in the upper right corner of each map. The wavelet transform was computed using 1Hz SNR data then downsampled to 10s for gridding purposes.

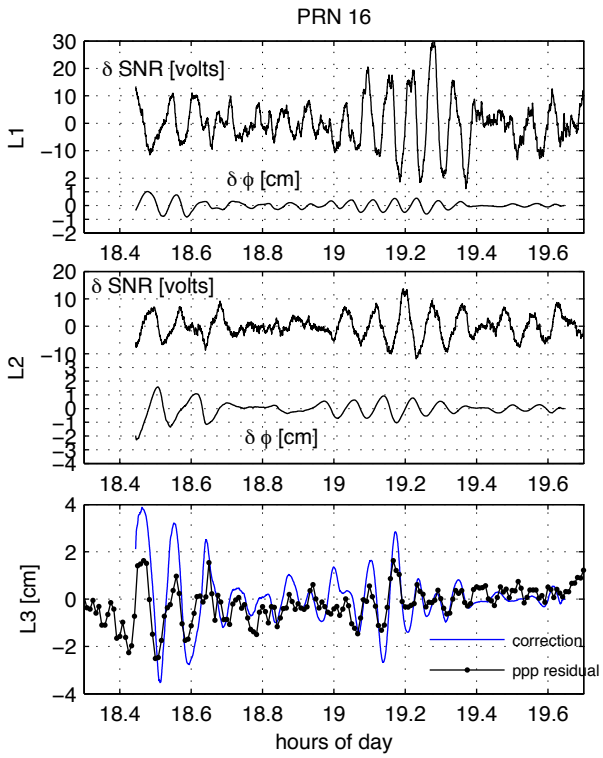

Figure 7: SNR data and phase multipath modeling results from the ascending portion of a pass of PRN16, CHUR, 2006 August 1. The SNR due to multipath (δSNR) and the derived phase correction ($\delta\phi$) are shown for both L1 and L2 frequencies; δSNR data are smoothed with a 7-point boxcar. Single-frequency corrections are joined using the ionosphere-free L3 data combination for direct comparison with 30s point positioning phase residuals. SNR data below 4V were thrown out [Tom Meehan, personal communication].

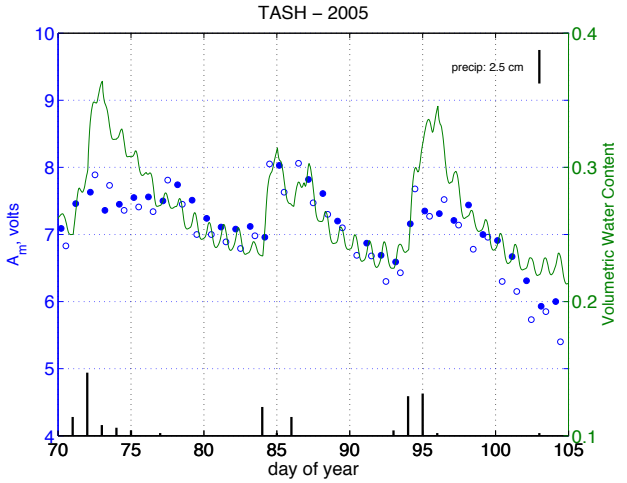

Figure 8: Comparison of GPS multipath amplitudes and modeled volumetric water content. Open circles are PRN1 and closed circles are PRN9, both of which reflect from the same section of ground for the analyzed SNR data. Black bars are daily precipitation values from a nearby airport. Reproduced from *Larson et al.* [2007] with permission of the authors.

SNR OF DOUBTFUL UTILITY

This section explores the SNR data quality of several receiver models commonly used by geodesists and present in permanent geodetic networks. All of the receivers discussed are dual frequency models, thus allowing analysis of SNR on both GPS frequencies. We draw our examples from continuously-operating GPS stations from a variety of networks; unless otherwise noted, these data are drawn from the SOPAC and CDDIS (http://garner.ucsd.edu/; ftp://cddis.gsfc.nasa.gov/pub/gps) archives. These examples are provided only to establish patterns of SNR reporting; the potential causes of low SNR quality are not explored in-depth.

One significant issue is precision of the reported SNR data; we note that several receiver models report SNR measurements in 1.0 dB-Hz increments (Figure 9). These include several Ashtech (micro-Z, Z-18), JPS (Legacy, E-GGD), and Leica (CRS1000, RS500, SR520) models. As shown in Figure 9, the 1.0 dB increments lead to a stairstep pattern in the SNR time series. The discrete nature of these SNR values obscures the multipath signature so that its power and frequency content cannot be easily assessed with spectral analysis techniques. Thus, without increased precision, the SNR data cannot be used for applications such as power spectral mapping, phase multipath modeling, or soil moisture studies.

Bilich [2006] determined that some receiver models exhibit apparent oscillations in SNR which appear to be unrelated to the multipath environment. The recent models of Trimble receivers, namely the 4700, 5700, and NetRS models, fall into this category. In each of the examples provided (Figure 10), the L1 data have very large amplitude oscillations, but no such oscillations are visible in the L2 data. Based upon the SNR theory outlined above, multipath should affect both L1 and L2 signals with similar amplitudes but different frequencies of oscillation. The lack of contemporaneous oscillations of similar amplitude in the L2 SNR indicates these apparent L1 oscillations are actually some kind of reset or dropout in SNR computation or reporting. The S1-S2 disparities are most apparent at the satellite's apex towards the center of each time series (Figure 10) where multipath amplitude should be small compared to low-elevation data. The older Trimble 4000-series receivers sometimes contain similar dropouts on S1 (Figure 11), but these dropouts occur almost exclusively at the high elevation angles where multipath magnitude is small.

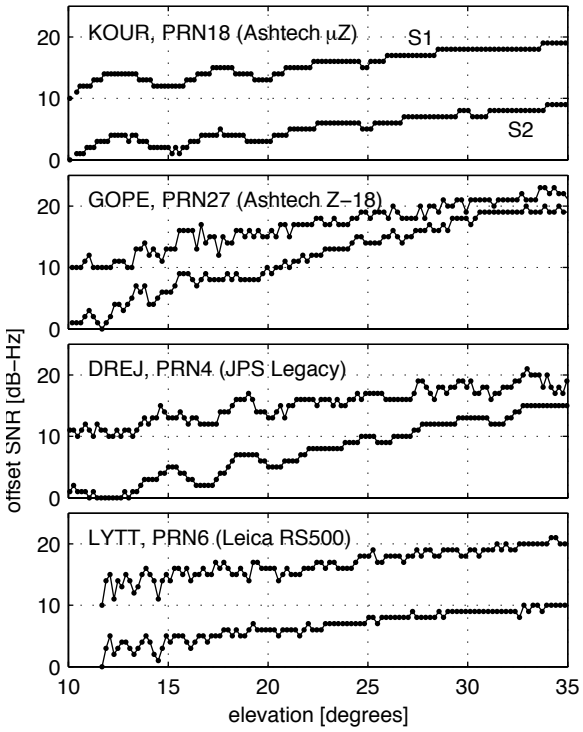

Figure 9: SNR values recorded for different satellites and stations on 2005 August 16; the SNR on both L1 and L2 GPS frequencies is given, where the recorded values are depicted by dots and traces are offset for clarity. All of the receiver types shown here report SNR values in 1.0 dB-Hz increments, and all data are sampled at 30s intervals.

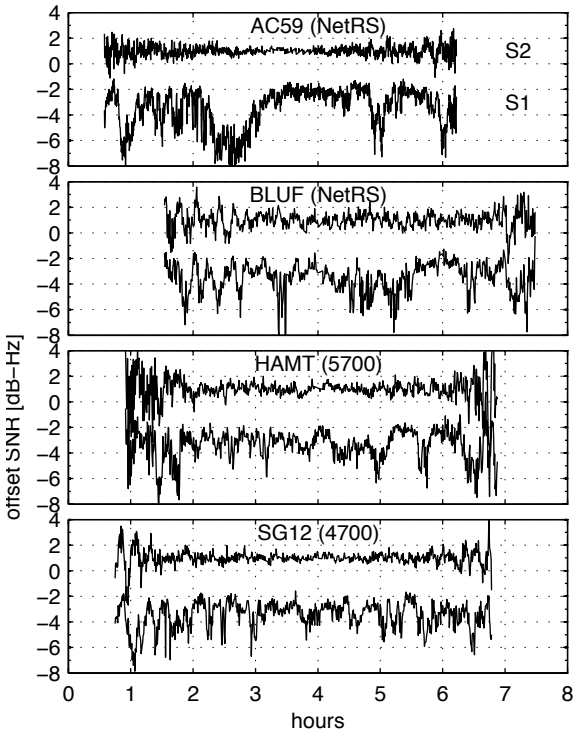

Figure 10: SNR values for PRN23, 2005 August 16, as reported by recent-model Trimble receivers operating at 4 different stations. In each plot, the top trace is the L2 SNR and bottom is the L1 SNR where a 7-13 order polynomial has been removed from each timeseries to account for the direct signal amplitude; the Trimble receiver model given in parentheses.

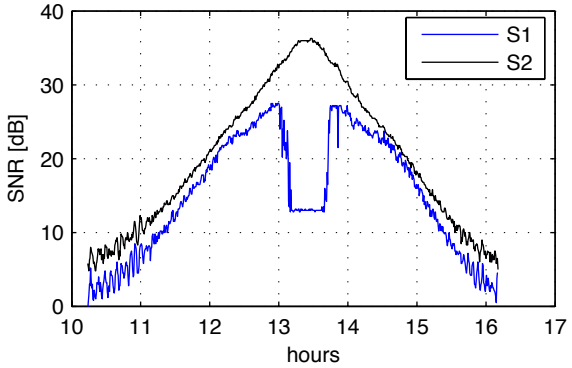

Figure 11: SNR data for a full arc of PRN22 as observed by a Trimble 4000 receiver at HARB on 2005 January 1; the S1 data have been offset by –5 dB for clarity.

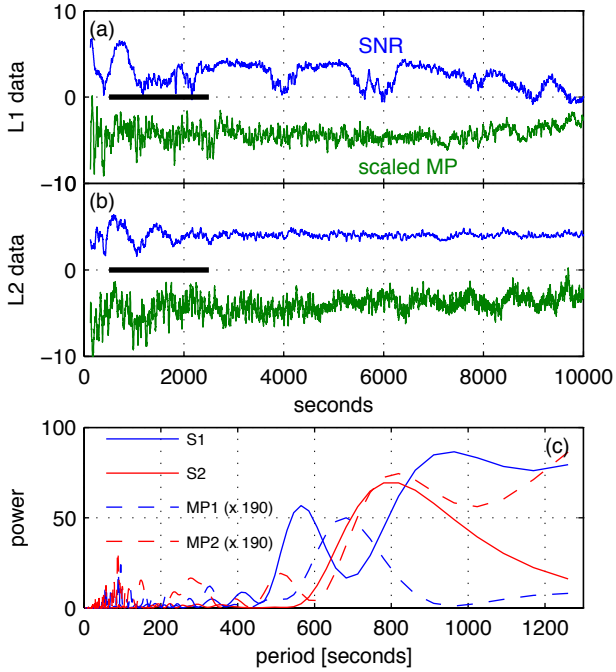

Figure 12: SNR and code multipath combination data from the ascending arc of PRN23 as observed at SG01 on 2007 February 6. On this date, SG01 was using a Trimble 4700 receiver operating at 1-Hz; all data for L1 (a) and L2 (b) were lowpass filtered for >15s periods and MP have units of meters (scaled x10). (c) spectral power of the data marked by the heavy line in (a-b), which cover 12-22° elevation.

These large-amplitude changes in the S1 time series for recent model Trimble receivers create two issues -- apparent oscillations which could be misconstrued as a multipath signal, and offsets of sufficient magnitude and noise level to obscure the true multipath oscillations. An example from SG01, a SuomiNet station temporarily changed to a 1-Hz data rate for this study, demonstrates these issues. The SG01 monument is a concrete pillar in a flat field with ~1.55m antenna-ground height [John Braun, personal communication], thus we expect to see slow oscillations in both S1 and S2 at low elevation angles, similar to CHUR (Figure 5). As shown in Figure 12, the S2 data display the expected slow, large-amplitude oscillations at the end of the arc but in the S1 data this signature is severely modified by the offsets. Without previous knowledge of the multipath environment, an analyst might mistake the S1 oscillations (actually, dropouts) at higher elevation angles as a multipath signature. The S2 data display low-elevation oscillations with the same frequency as MP2 (Figure 12c), but the pseudorange noise and smoothing effects on the MP combination make it difficult to confirm these data types are also in-phase (correlation is moderate).

Some receivers exhibit a strong coupling between S1 and S2 tracking errors, demonstrated by S2 timeseries that are of similar frequency to and largely in-phase with S1 timeseries. Ashtech Z-12 receivers, which are very common in CGPS networks operating at a variety of sample rates, exhibit these characteristics. Consider an example from MKEA, a 1-Hz station on the flanks of Mauna Kea volcano in Hawaii. As shown in *Bilich and Larson* [2007], this station experiences very high frequency multipath with signals reflected from adjacent cinder cones. The high frequencies (< 200s periods; > 0.005 Hz) enable analysis of SNR and MP data types over a short time window where the range of satellite elevation angles is small, so that multipath frequency ω is relatively constant and is easily resolved. From visual inspection alone, the S1 and S2 data appear to be completely in-phase with identical frequency content (Figure 13a-c). However, concentrating on a small 500s section of data it is apparent that S2 contains two dominant frequencies, one frequency equivalent to the S1 frequency and one which obeys the assumed S1/S2 ratios of decoupled SNR data, i.e. $f_{S1}/f_{S2} \approx 1.28$ (Figure 13d). For these high magnitude multipath data with a clear multipath signature in the pseudorange multipath combination, a fairly robust correlation exists between SNR and MP on both frequencies. However, the coupling of S2 to S1 data indicates that the S2 data type cannot be reliably used for scientific analysis.

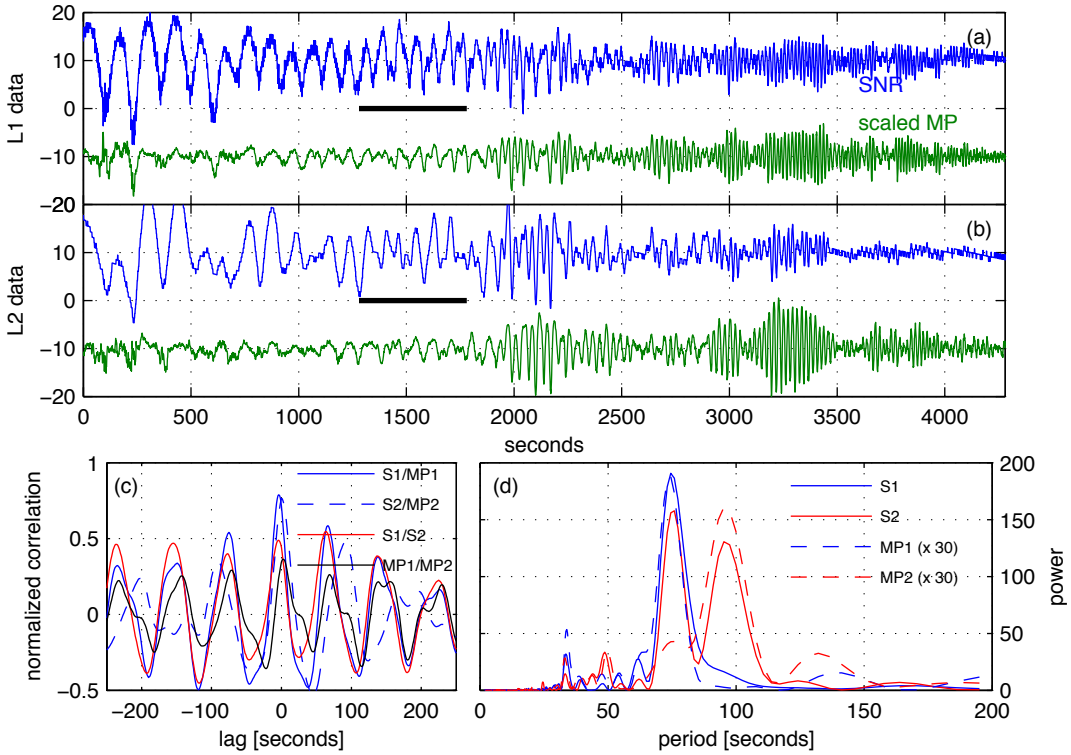

Figure 13: SNR and code multipath combination data from the ascending arc of PRN1 as observed at MKEA on 2005 August 15 with an Ashtech Z-12 receiver operating at 1-Hz. MP data have units of meters (scaled x2); see Figure 4 for subplot explanations. Plots (c) and (d) use the 500s of data marked by the heavy line in (a-b), which cover 22.6-25.9° elevation.

A large number of CGPS stations worldwide use pillar or tripod monument construction with an antenna-ground distance of 1.5-2.0 m, resulting in slow, large magnitude oscillations when signals are reflected from flat ground underneath an antenna. For this type of multipath environment, the coupling of S1 and S2 Ashtech Z-12 data appears to be more severe. In Figure 14 we provide an example of ground-reflection multipath from experimental data collected on Marshall Mesa in Boulder, Colorado (39.9°N, 105.2°W, 1729m) in a very flat field. The SNR data appear to be perfectly in-phase with nearly identical amplitudes, yet the spectra show slightly different frequencies with a S1/S2 ratio closer to 1.1 than the desired 1.28 and a very broad S2 peak. These spectra indicate S1 and S2 are still coupled but do not have the distinct dual peaks observed in the higher frequency data.

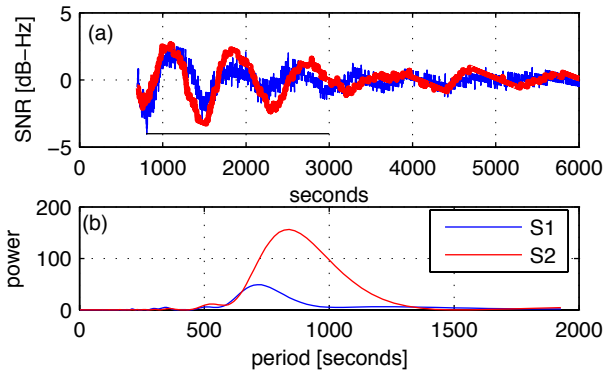

Figure 14: (a) Dual-frequency Ashtech Z-12 SNR data collected at Marshall Mesa on 2007 July 22 with a ~ 1.6m tall antenna; the heavy line brackets the data for the spectral power estimate in (b).

This leaves only a few geodetic GPS receivers with the desired high precision and accuracy of SNR measurements. However, some of these same receivers have SNR data which fail to correlate properly with the pseudorange multipath combination (Equations 1 and 3; Table 1), casting doubt upon their accuracy and the link between these SNR and the carrier phase tracking loop. Many receivers implement carrier smoothing of the pseudorange by default, and this smoothing may change the character of the MP observable combination so that it is difficult to draw definitive conclusions from SNR and MP correlations. Thus our best check of SNR dependence on the simplified multipath model is tenuous at best.

In an attempt to define trends in SNR and MP correlations, *Bilich* [2006] computed average SNR-MP correlations for 525 permanent GPS stations and 11 different receiver models. The correlation study used all stations in the SOPAC archive (ftp://garner.ucsd.edu) with SNR data on 2002 August 16, and used data from all arcs in the 15-25° elevation range. Figure 15 summarizes the correlation study in terms of the averaged normalized correlation value at zero lag. In this figure, well-correlated SNR and MP values will have a large mean correlation value with a peak over to the right of the plot (unity correlation at zero lag) whereas poorly-correlated values have short peaks clustered near the left (zero correlation at zero lag). This analysis indicates that AOA ACT receivers are well-correlated for both L1 and L2 frequencies, while AOA TurboRogue, Ashtech Z-12, and Trimble 4000 receivers have moderate correlations on the L1 frequency only. Trimble NetRS receivers showed a moderate correlation on L2, but dropouts in S1 data made L1 correlation testing difficult and inconclusive.

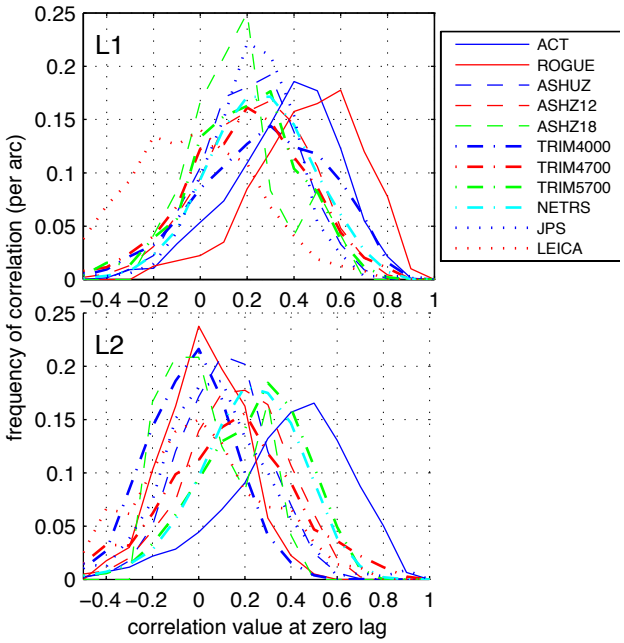

Figure 15: SNR and multipath correlation statistics for various receiver models. The ordinate is the value of the normalized (i.e. maximum = 1.0) correlation at zero lag, and the abcissa is a statistic indicating how often each correlation value occurs. Well-correlated SNR-MP data will result in large correlation values (peak to the right-hand side of plot) occurring often (tall peak).

CONCLUSIONS

Accurate SNR measurements from some types of geodetic receivers have been shown to provide a valuable new addition to the GPS observation set for scientific applications. This paper has presented examples of the application of SNR measurements to screen and improve carrier phase data for subsequent positioning analysis and a recently developed technique to use these data directly for sensing soil moisture variations.

Unfortunately, not all commonly used geodetic receivers provide the requisite precision and accuracy for such applications (Table 2). We conclude that AOA ACT receivers have dual-frequency SNR data of sufficient precision and accuracy, while Ashtech Z-12 receivers have precise and accurate SNR data on the L1 frequency only; all other receiver models studied have one or more

questionable characteristics that limit their applicability in the example techniques. We hope that in identifying useful characteristics of these measurements, we might encourage manufacturers of receivers for scientific applications to improve the quality of this previously underutilized measurement type.

ACKNOWLEDGMENTS

The authors would like to thank IGS, SOPAC, JPL, CDDIS, NASA, and UNAVCO for infrastructure and archiving support, and John Braun for collecting high-rate data at SG01. This research was sponsored by grants from NSF (EAR-0003943, EAR-0337206) and NASA (SENH 154-0351) and a NSF graduate student research fellowship (AB).

REFERENCES

Axelrad P, Larson KM, Jones B (2005) Use of the correct satellite repeat period to characterize and reduce site-specific multipath errors. In: *Proceedings of ION GNSS 2005*, Long Beach, CA.

Bilich A (2006) Improving the precision and accuracy of geodetic GPS: Applications to multipath and seismology, Ph.D. dissertation, University of Colorado

Bilich A, KM Larson, P Axelrad (2007) Modeling GPS phase multipath with SNR: Case study from the salar de Uyuni, Boliva. Under review at *Journal of Geophysical Research*, available at http://xenon.colorado.edu/Papers/salarUyuni_2007JB005194.pdf

Bilich A, KM Larson (2007) Mapping the GPS Multipath Environment Using the Signal-to-Noise Ratio (SNR). Accepted by *Radio Science*; available at http://xenon.colorado.edu/Papers/MultipathMaps_2007RS003652.pdf

Ward P (1996) Satellite signal acquisition and tracking. In: *Understanding GPS: Principles and Applications*, ed. E. D. Kaplan, Artech House.

Braasch MS (1996) Multipath effects. In: *Global Positioning System: Theory and Applications*, edited by B. W. Parkinson, J. J. S. Jr., P. Axelrad, and P. Enge, vol. 1, chap. 14, American Institute of Aeronautics and Astronautics.

Comp C, Axelrad P (1997) Adaptive SNR-based carrier phase multipath mitigation technique, *IEEE Transactions on Aerospace and Electronic Systems 34* (1): 264-276. DOI 10.1109/7.640284

Estey LH, CM Meertens (1999) TEQC: The multi-purpose toolkit for GPS/GLONASS data, *GPS Solutions 3*: 42-49.

Gurtner W, G Mader (1990) Receiver Independent Exchange Format Version 2, *CSTG GPS Bulletin 3*.

Georgiadou Y, Kleusberg A (1988) On carrier signal multipath effects in relative GPS positioning. *Manuscripta Geodaetica*, 13:172-179

Larson KM, EE Small, E Gutmann, A Bilich, P Axelrad (2007) Using GPS multipath to measure soil moisture fluctuations: Initial results. *GPS Solutions*, doi:10.1007/s10291-007-0076-6.

Ray JK (2000) Mitigation of GPS code and carrier phase multipath effects using a multi-antenna system. Ph.D. dissertation, University of Calgary

Torrence C, Compo GP (1998) A practical guide to wavelet analysis, *Bulletin of the American Meteorological Society, 79*, doi:10.1175/1520-0477.

Table 2: Summary of SNR characteristics and level of SNR/MP correlation for the receiver models examined in this study. Grayed-out sections of the table denote relationships which were not tested in this study.

	Undesirable SNR Characteristics			*SNR/MP Correlation*		
Receiver Model	*Coarse Increments*	*Dropouts*	*In-phase S1/S2*	*High*	*Moderate*	*Low*
AOA ACT				L1 & L2		
Ashtech Z-12			X		L1 & L2	
Ashtech microZ/Z-18	X					
Trimble 4000		X			L1	L2
Trimble 4700/5700/NetRS		X			L2	
Leica	X					
Javad/JPS	X					